Journal of Power Sources 195 (2010) 5109–5113

Contents lists available at ScienceDirect

Journal of Power Sources

journal homepage: www.elsevier.com/locate/jpowsour

Short communication

Assembly of CdSe onto mesoporous TiO_2 films induced by a self-assembled monolayer for quantum dot-sensitized solar cell applications

Lai-Wan Chong, Huei-Ting Chien, Yuh-Lang Lee*

Department of Chemical Engineering, National Cheng Kung University, No. 1 University Road, Tainan 70101, Taiwan, ROC

ARTICLE INFO

Article history:
Received 30 October 2009
Received in revised form
26 December 2009
Accepted 21 January 2010
Available online 1 February 2010

Keywords:
Quantum dots-sensitized solar cells
CdSe
Self-assembly monolayer
3-Mercaptopropyl-trimethyoxysilane
Surface modification

ABSTRACT

A self-assembled monolayer (SAM) of 3-mercaptopropyl-trimethyoxysilane (MPTMS) is pre-assembled onto a mesoporous TiO_2 film and is used as a surface-modified layer to induce the growth of CdSe QDs in the successive ionic layer adsorption and reaction (SILAR) process. Due to the specific interaction of the terminal thiol groups to CdSe, the MPTMS SAM is found to increase the nucleation and growth rates of CdSe in the SILAR process, leading to a well covering and higher uniform CdSe layer which has a superior ability, compared with the electrode without MPTMS, in inhibiting the charge recombination at the electrode/electrolyte interface. Furthermore, the performance of the CdSe-sensitized TiO_2 electrode can further be improved by an additional heat annealing after film deposition, attributable to a better interfacial connection between CdSe and TiO_2, as well as a better connection among CdSe QDs. The CdSe-sensitized solar cell prepared by the present strategy can achieve an energy conversion efficiency of 2.65% under the illumination of one sun (AM 1.5, 100 mW cm^{-2}).

1. Introduction

Dye-sensitized solar cells (DSSCs) are operated based on photosensitization of mesoporous TiO_2 films using organic sensitizers which can harvest sun light. The performance of a DSSC is intimately controlled by the sensitizer adsorbed on the TiO_2 surface. By using sensitizers of ruthenium complexes, energy conversion efficiency up to 11% has been achieved [1]. The high efficiency of the DSSC, as well as its characteristics of low cost and surrounding friendly, makes DSSC a promising alternative to conventional solid-state solar cells.

In addition to the organic sensitizers commonly used for DSSCs, inorganic semiconductors which absorb visible light can also be used as light harvesters of DSSCs. Quantum dots (QDs) metal chalcogenide semiconductors such as CdS [2,3], CdSe [4], PbS [5,6], and PbSe [7] have received interest in this application. The advantage of QDs sensitizers includes the impact ionization and Auger recombination caused from quantum confinement effect. These effects are known to increase the exciton concentration, life-time of excited electrons, quantum yield, and therefore, the performance of a QD-sensitized solar cell (QD-SSC).

Despite QDs have specific advantages over organic materials to be the sensitizers of DSSCs, there are relatively fewer studies devoted to the QD-sensitized solar cells (QD-SSCs), and their energy conversion efficiencies are still low. One of the reasons leading to the poor performance of QD-SSCs is the difficult in assembling QDs into the mesoporous TiO_2 matrix to obtain a well-covering QD layer on the TiO_2 crystalline surface. It also happened that the deposited QDs may block the entrance of pores, under inappropriate deposition conditions, and therefore, the electrolyte cannot contact the QDs inside the pore. Two methods were commonly used to assemble QDs into a mesoporous thin film. The first is assembling pre-prepared QDs using bifunctional linkers [8], and the other is an in situ deposition from their precursor solutions using successive ionic layer adsorption and reaction (SILAR) process. In our previous papers, various methods were proposed to deposit CdS into a TiO_2 film including inducing the growth of CdS or CdSe in the SILAR process by using a pre-assembled seed layer of QDs, and modifying the SILAR process performed in an alcohol system. These methods have proved to be efficient in improving the performance of QD-SSCs and the energy conversion efficiency achieved by CdS-SSC and CdSe-SSC were 1.15 [9] and 1.4% [10], respectively. By using a CdS/CdSe co-sensitized TiO_2 electrode, efficiency as high as 4.22% was achieved [11].

Among various semiconductor sensitizers reported in the literature, CdS and CdSe appeared to have better performance in comparison with other materials. Comparing between CdS and CdSe, CdS has a band gap of 2.25 eV in bulk which limits its absorption range below the wavelength of ca. 550 nm. For the CdSe, its smaller band gap (1.7 eV) leads to a wider absorption range (below ca. 730 nm) which is more advantageous to be a sensitizer of a photoelectrode. However, the incident photon to current conver-

* Corresponding author. Tel.: +886 6 2757575x62693; fax: +886 6 2344496.
E-mail address: yllee@mail.ncku.edu.tw (Y.-L. Lee).

0378-7753/$ – see front matter © 2010 Elsevier B.V. All rights reserved.
doi:10.1016/j.jpowsour.2010.01.044

sion efficiencies (IPCE) reported for CdSe-SSC is smaller than that for CdS-SSC [11]. It was also found that the growth rate of CdSe in the SILAR process is much lower than that of CdS. The low growth rate of CdSe is probably associated with the lower IPCE of the CdSe-SSC because a low deposition rate usually implies a poor interaction of a deposited layer (CdSe) to the substrate (TiO_2). To explore this issue and to enhance the performance of CdSe-SSC, a 3-mercaptopropyl-trimethyoxysilane (MPTMS) monolayer was pre-assembled onto the TiO_2 surface. The terminal thiol groups of MPTMS layer is supposed to trigger a better interaction of the TiO_2 film to CdSe, inducing the growth rate of CdSe in the subsequent SILAR process. This strategy was proved to be efficient to the growth of CdSe and to the performance enhancement of a CdSe-SSC.

2. Experimental

Mesoscopic TiO_2 films were prepared by spin coating of TiO_2 paste (Degussa P25) on indium-doped tin oxide (ITO, about 13 $\Omega\,\square^{-1}$, Solaronix SA) substrates, followed by sintering at 450 °C for 30 min. The thickness of the TiO_2 film was measured to be 11 μm. TiO_2 films were surface-modified by immersing in a 1 wt.% MPTMS/toluene solution for 5 min. After that, the following SILAR process of CdSe, sodium selenosulphate (Na_2SeSO_3) was used as the Se source. The Na_2SeSO_3 aqueous solution was prepared by refluxing Se (0.05 M) in an aqueous solution of Na_2SO_3 (0.05 M) at 70 °C for 7 h. In the SILAR process of CdSe, the SAM-modified TiO_2 substrate (or bare TiO_2) electrode was dipped first into an ethanol solution containing $Cd(NO_3)_2$ (0.05 M) for 5 min at 50 °C, rinsed with ethanol, and then dipped into a Na_2SeSO_3 solution for 20 min at 50 °C, and rinsed again with pure water. The two-step dipping procedure is termed as one SILAR cycle. Repeating the SILAR cycle would increase the incorporated amount of CdSe. The SILAR method was also used to deposit the ZnS passivation layer. The electrode was dipped sequentially into a 0.5 M $Zn(NO_3)$ ethanol solution and a 0.5 M Na_2S methanol solution. The optimal dipping time was found to be 1 min for both solutions. After that, the electrodes were heated annealing at 150 °C for 30 min or 300 °C for 2 min. A QD-SSC was assembled by sandwiching a sensitized TiO_2 photoelectrode and an Au-coated counter electrode using 60 μm thick sealing material (SX-1170-60, Solaronix SA). A polysulfide electrolyte prepared using water/methanol (7:3 by volume) solution was used in this work. The electrolyte contains 0.5 M Na_2S, 0.1 M S, and 0.2 M KCl. The active area of the cell was 0.16 cm^2.

The photocurrent–voltage (*I–V*) curves were measured under an illumination of a solar simulator (Newport, Oriel class A, 91160A) at one sun (AM 1.5, 100 mW cm^{-2}). An Eco Chemie Autolab potentiostat/galvanostat was used to record the current–voltage (*I–V*) characteristics. An Oriel 500 W xenon arc lamp and Keithley 2400 electrometer were used during the measurements of IPCE. Electrochemical impedance spectra (EIS) were measured under the illumination of AM 1.5 100 mW cm^{-2} by applying an oscillation potential of 10 mV from 10^{-2} to 10^5 Hz. A potentiostat equipped with a frequency response analyzer (Autolab, PGSTAT 30 and FRA2 module) was used in this analysis.

3. Results and discussion

CdSe was deposited on MPTMS-modified and bare TiO_2 films, and the prepared CdSe-sensitized electrodes were termed as TiO_2/MPTMS/CdSe and TiO_2/CdSe, respectively. The incorporated amount of CdSe in a TiO_2 film was evaluated using the absorbance of UV–vis spectrum. Fig. 1 shows the spectra of CdSe-sensitized TiO_2 electrodes prepared using various SILAR cycles. It is found that the absorbance of TiO_2/MPTMS/CdSe is higher in comparison with that of TiO_2/CdSe electrode at the same SILAR cycle, indicating that

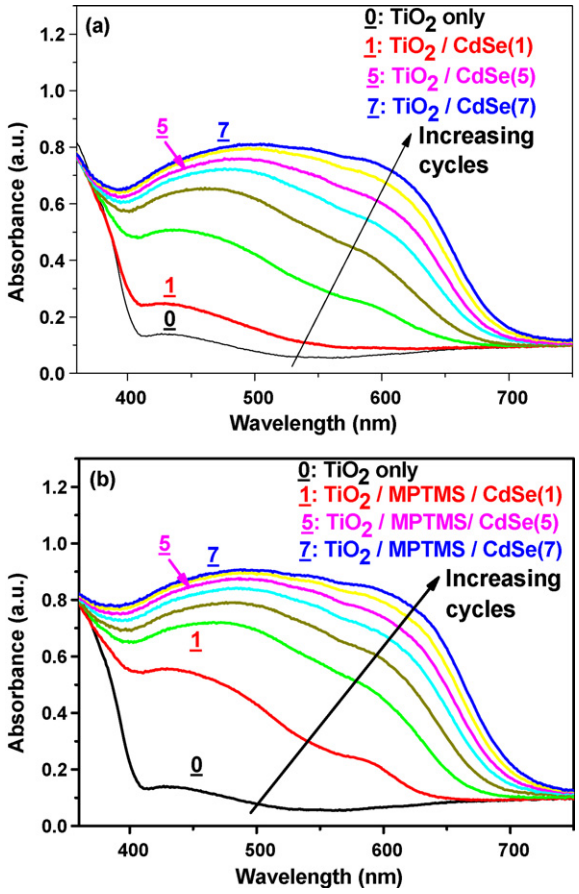

Fig. 1. UV–vis absorption spectra of CdSe-sensitized TiO_2 film prepared by various cycles of SILAR process performed on bare TiO_2 an electrode (a), or an electrode surface-modified by MPTMS (b). The number on each curve corresponds to the SILAR cycle introduced to assemble the CdSe.

higher amount of CdSe was deposited on MPTMS-modified TiO_2. This phenomenon is especially obvious in the early SILAR cycles, which implies that the presence of MPTMS SAM has a growth-enhancing effect to the subsequent deposition of CdSe.

Because the week adhesion of CdSe on TiO_2 surface, CdSe are likely to desorb from TiO_2 surface while rinsing by its solvent at each SILAR cycle, leading to a low deposition amount of CdSe per SILAR cycle. Therefore, the TiO_2 surface is partially covered by CdSe clusters of low density, which act as nucleation sites in the following growth of CdSe. Due to the low density of CdSe clusters formed in the initial SILAR cycle, it is difficult to get a well-covered TiO_2 surface by increasing the deposition cycle. CdSe nanocrystallites could grow large and block the mesopores before TiO_2 surface was completely covered by CdSe.

For the MPTMS-modified TiO_2 film, the presence of thiol terminal groups helps incorporating and stabilizing CdSe, decreasing the desorption events of CdSe while rinsing, and thereby, increasing the deposition amount of CdSe in the first cycle. Densely distributed CdSe clusters were anticipated to form on the MPTMS-modified TiO_2 film. In the subsequent SILAR cycles, the high-density CdSe clusters trigger a better covering and more uniform CdSe layer on the TiO_2 surface.

Increasing SILAR cycle, the absorbance increases steadily with a slight red-shift of the absorption shoulder and onset position. The absorption edge of a photoelectrode can be measured from the intersection of the baseline with the tangent line of the sharply decreasing region of an absorption spectrum. For the photoelectrode with the best performance in energy conversion efficiency (η),

Table 1
Parameters obtained from the photo current–voltage (*I–V*) measurement of the bare and MPTMS-modified DSSCs.

Structure	I_{sc} (mA cm^{-2})	V_{oc} (mV)	FF	η (%)
TiO_2/CdSe(1)	1.72	445	0.37	0.28
TiO_2/CdSe(2)	2.66	501	0.38	0.51
TiO_2/CdSe(3)	4.80	515	0.36	0.88
TiO_2/CdSe(4)	6.40	515	0.37	1.22
TiO_2/CdSe(5)	8.47	493	0.36	1.50
TiO_2/CdSe(6)	7.43	374	0.37	1.04
TiO_2/MPTMS/CdSe(l)	4.18	492	0.50	1.03
TiO_2/MPTMS/CdSe(2)	5.53	504	0.47	1.31
TiO_2/MPTMS/CdSe(3)	6.47	499	0.46	1.48
TiO_2/MPTMS/CdSe(4)	7.09	481	0.47	1.61
TiO_2/MPTMS/CdSe(5)	8.43	470	0.46	1.80
TiO_2/MPTMS/CdSe(6)	8.53	454	0.46	1.78

TiO_2/MPTMS/CdSe(5), the measured absorption edge is ca. 694 nm, corresponding to a band gap of 1.79 eV. The mean size of CdSe particles estimated from the excitonic peak is 5.9 nm [12,13]. For the TiO_2/CdSe(5) electrode, the measured absorption edge and band gap are 684 nm and 1.81 eV, respectively, and the mean particle size is 5.4 nm. These results indicate that the sizes of CdSe are in the range of QDs and, furthermore, the MPTMS-modified electrode has a smaller band gap and larger particle sizes compared with the unmodified TiO_2 film.

CdSe-sensitized TiO_2 photoelectrodes were prepared using various SILAR cycles and used to assemble CdSe-sensitized solar cells (CdSe-SSCs). The photocurrent–voltage (*I–V*) curves for the CdSe-SSCs were measured under the illumination of one sun (AM 1.5, 100 mW cm^{-2}). The open circuit potential (V_{oc}), short circuit current (I_{sc}), fill factor (FF), and the total energy conversion efficiency (η) of these cells were summarized in Table 1. For the electrodes prepared by only 1 SILAR cycle, the efficiency η is 0.28% for the TiO_2/CdSe(1) cell, but a much higher value, η = 1.03%, is obtained for the MPTMS-modified cell, TiO_2/MPTMS/CdSe(1). This result is attributed to the higher incorporation amount and better coverage CdSe on MPTMS-modified TiO_2 surface, which leads to higher values of I_{sc}, V_{oc}, and FF of the MPTMS-modified cell. With increase of SILAR cycles, the overall efficiency increases first, and then decreases after reaching a maximum value. The efficiency increase in the early SILAR cycles is mainly caused by the increase of I_{sc}, which is consistent to the increasing amount of CdSe incorporated to the photoelectrode. The maximum efficiency obtained for the MPTMS-modified (TiO_2/MPTMS/CdSe) and unmodified (TiO_2/CdSe) TiO_2 electrodes are 1.80 and 1.50%, respectively, both occur at the electrodes prepared by 5 SILAR cycles.

It is noteworthy that the fill factors (FFs) vary little with SILAR cycles and, furthermore, the FFs measured for the TiO_2/MPTMS/CdSe cells (ca. 0.46) are higher than those of the TiO_2/CdSe cells, which is responsible for the higher efficiency of the MPTMS-modified cells. It is inferred that the presence of MPTMS SAM layer itself and the better coverage of CdSe film on the MPTMS–TiO_2 surface reduces the direct contact of TiO_2 to the electrolyte, preventing the recombination of excited electrons from the conduction band of TiO_2 to the electrolyte, and thereby, leading to the higher FF. This inference was sustained by the *I–V* characteristics of the cells measured under dark conditions (Fig. 2). Furthermore, electrochemical impedance spectroscopy (EIS) analysis was also conducted to measure the charge recombination resistances (R_r) at the electrode/electrolyte. Fig. 3a shows the typical Nyquist plots obtained at an applied voltage of 0.3 V under light illumination of one sun (AM 1.5, 100 mW cm^{-2}). The second semicircle of an EIS spectrum was associated with the chemical capacitance of nanostructured TiO_2 (C_μ) and the R_r of a measured condition. By using the equivalent circuit shown in Fig. 3a [14,15],

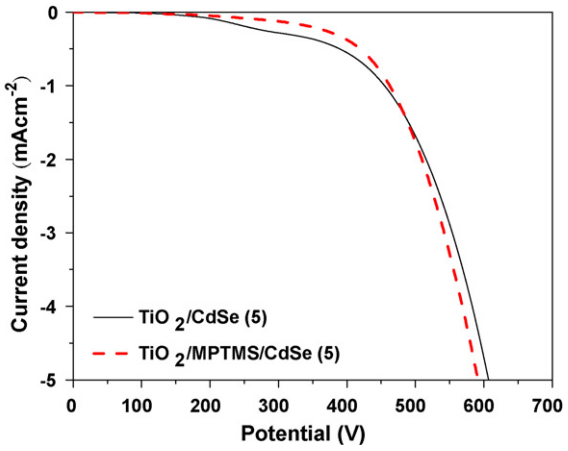

Fig. 2. *I–V* characteristics of the bare and SAM-modified cells measured under dark conditions.

the recombination resistances at various applied potentials can be measured. These results are shown in Fig. 3b for TiO_2/MPTMS/CdSe and TiO_2/ CdSe electrodes.

Fig. 3(b) shows that the recombination resistance (R_r) decreases with increase of applied potential for both electrodes, consistent with the results reported in the literature for quantum dot-sensitized solar cells [15]. Comparing between the two electrodes, the recombination resistance measured for the TiO_2/MPTMS/CdSe is smaller at low applied voltages, but higher at the higher volt-

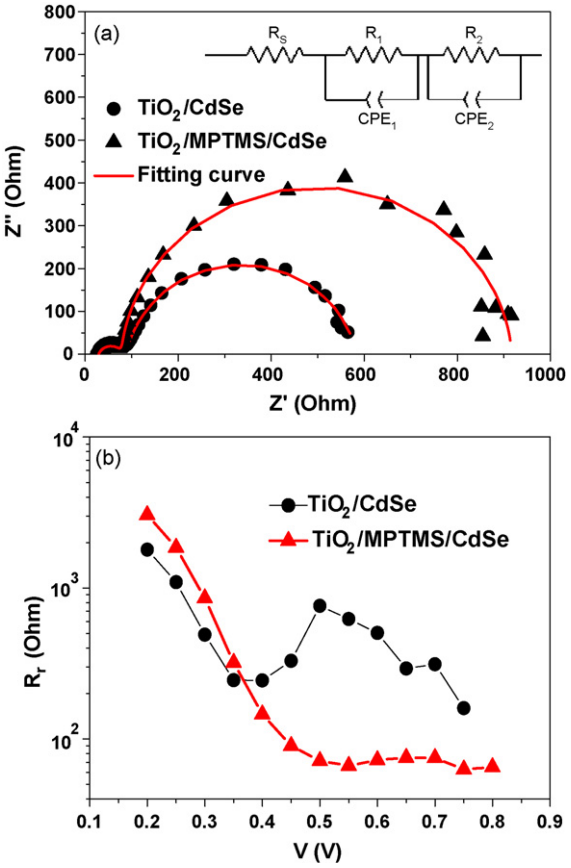

Fig. 3. (a) Nyquist plots of EIS spectra measured under light illumination of one sun (AM 1.5, 100 mW cm^{-2}) for the bare and SAM-modified cells. The measurement was performed at an applied voltage of 0.3 V. (b) The electron recombination resistance, Rr, as a function of applied voltage. The insect in (a) shows the equivalent circuit employed to measure the resistance.

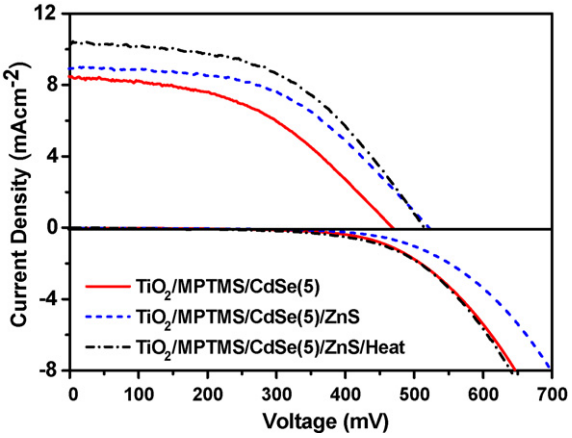

Fig. 4. *I–V* characteristics of the various CdSe-sensitized DSSCs measured under the illumination of one sun (AM 1.5, 100 mW cm^{-2}). The *I–V* characteristics of the cells measured under dark conditions are shown in the lower part of this figure.

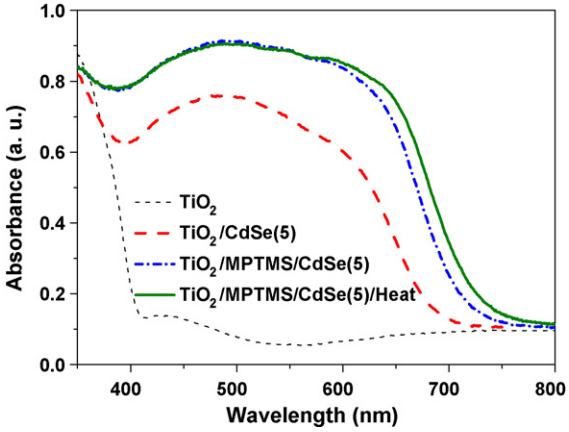

Fig. 5. UV–vis absorption spectra of CdSe-sensitized TiO_2 film with and without heat annealing at 300 °C for 2 min.

ages. This result is consistent with the dark currents shown in Fig. 2, which demonstrates that the dark current of the TiO_2/MPTMS/CdSe is smaller and higher, respectively, at low and high potential range. This result implies that the presence of MPTMS SAM triggers an interfacial structure with superior ability in inhibiting charge recombination at low driving potential. However, at high-applied voltages, the recombination resistance of the TiO_2/MPTMS/CdSe electrode is relatively smaller. At low applied voltages, the higher R_r of TiO_2/MPTMS/CdSe can reasonably attributed to the better coverage of CdSe film and the passivation effect MPTMS SAM itself. With increasing of applied voltage, it is inferred that the electrons in the TiO_2/MPTMS/CdSe electrode will accumulate at the TiO_2/MPTMS interface due to the blocking effect of MPTMS layer. The accumulated electrons will charge the surface state, trigger a band unpinning, induce electron recombination through a monoenergetic surface state, and therefore, lead to a significant decrease of R_r at high potential range [15].

Although the recombination resistances of the two electrodes have different relationship at low and high potential ranges, the performances of the present cells are mainly controlled by the R_r measured at low potential range because the V_{oc} of the cells are generally smaller than 0.5 V (Table 1). That is, the MPTMS layer did trigger a higher charge recombination resistance in the operation of the TiO_2/MPTMS/CdSe cell.

It was reported that ZnS can be used as a passivation layer of CdS or CdSe to enhance the performance of a photoelectrode [16,17]. A ZnS layer was therefore assembled on the optimum electrode to prepare the TiO_2/MPTMS/CdSe/ZnS electrode. The *I–V* curves measured for the cells with and without a ZnS layer were shown in Fig. 4, and the related parameters were listed in Table 2. Compared with the device without ZnS, the I_{sc}, V_{oc}, and FF of the TiO_2/MPTMS/CdSe/ZnS increase due to the introduction of the ZnS layer and, therefore, the efficiency (η) increases from 1.80 to 2.29%. In order to clarify the role of ZnS, the *I–V* characteristics of the cells were measured under dark conditions and these results were shown in the lower part of Fig. 4. The dark current measured for the ZnS-modified cell is relatively smaller, demonstrating that the ZnS layer can inhibit the recombination of the excited electron at the electrode/electrolyte interface.

Table 2
Parameters obtained from the photo current–voltage (*I–V*) measurement of the DSSCs constructed by various electrodes.

Structure	I_{sc} (mA cm^{-2})	V_{oc} (mV)	FF	η (%)
TiO_2/CdSe	8.47	493	0.36	1.5
TiO_2/CdSe/ZnS	7.90	525	0.46	1.92
TiO_2/MPTMS/CdSe	8.43	470	0.46	1.8
TiO_2/MPTMS/CdSe/ZnS	8.86	523	0.50	2.29
TiO_2/MPTMS/CdSe/ZnS/heat	10.32	517	0.49	2.65

To further enhance the performance of the CdSe-sensitized TiO_2 electrode, the electrode was subjected to a heat annealing at 300 °C for 2 min. The heat-treated electrode was termed as TiO_2/MPTMS/CdSe/ZnS/Heat here after. The UV–vis spectra shown in Fig. 5 indicate that the heat annealing causes a slightly red-shift of the spectrum, implying that the sizes of CdSe QDs become larger after this treatment, probably due to necking and coalescence between QDs. The *I–V* characteristic and related parameters measured for the TiO_2/MPTMS/CdSe/ZnS/Heat cell was also shown in Fig. 4 and Table 2, respectively. It appears that the heat annealing triggers a significant increase of I_{sc} from 8.86 to 10.32 mA cm^{-2} which elevates the efficiency to 2.65%. These results are possibly attributed to the increase of the crystallinity of CdSe at a higher temperature, improve the charge transport characteristic of the photoelectrode, and, therefore, lead to a higher performance of the TiO_2/MPTMS/CdSe/ZnS/Heat cell.

The dark current measurement (shown in the lower part of Fig. 4) demonstrates that the dark current becomes higher after the heat treatment. This result seems consistent with the slightly decrease of V_{oc} and FF because a higher dark current implies a higher probability for the charge recombination at the electrode/electrolyte interface. However, a higher dark current also means a lower resistance for charge transfer in the CdSe layer, as well as at the TiO_2/CdSe interface. This result is reasonable because a heat annealing process is supposed to improve the interfacial connection between CdSe and TiO_2, as well as the connection among CdSe QDs. Therefore, an excited electron can efficiently move in the CdSe layer and inject into the TiO_2 matrix, which is responsible for the higher I_{sc} obtained for the heat-annealed device. Although the probability of charge recombination also increase due to the heat treatment, the enhancement in the electron collection (the I_{sc}) is much significant than the drawback caused by the charge recombination. Therefore, the energy conversion efficiency is increased.

The incident photon to current conversion efficiencies (IPCEs) of the cells were measured from the I_{sc} monitored at different excitation wavelengths and shown in Fig. 6. In general, the IPCE spectra of these cells are consistent with the corresponding UV–vis spectra shown in Fig. 5. The IPCEs of the cell without MPTMS (TiO_2/CdSe/ZnS) are less than 40%, but they increase up above 45% due to the introduction of a MPTMS SAM (TiO_2/MPTMS/CdSe/ZnS). Furthermore, a post-deposition heat annealing can further elevate the IPCE up above 50%. Comparison between devices with and with-

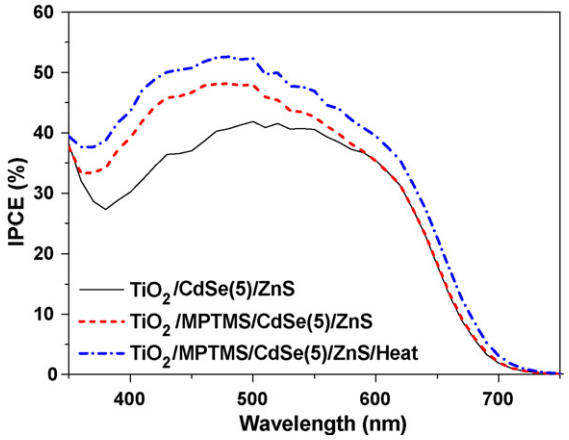

Fig. 6. Incident photon to current conversion efficiencies (IPCEs) of various electrodes measured as a function of wavelength.

out the heat annealing, the IPCE of the heat-annealed cell is ca. 10% higher than the cell without heat treatment, but the absorption edges of the IPCE spectra are similar. These results tell that the increase of I_{sc} after heat annealing is mainly caused by the efficient injection of excited electrons. The red-shift of the UV–vis spectrum after heat annealing has little effect in increase the light harvest range of the cell.

4. Conclusions

The present results show that the growth of CdSe in a mesoporous TiO_2 film can be assisted by a MPTMS SAM pre-assembled on the TiO_2 surface. The presence of MPTMS SAM induced a faster growth rate of CdSe in the SILAR process, leading to a better covering and more uniform CdSe layer which has superior ability in inhibiting the charge recombination at the electrode/electrolyte interface. Moreover, an additional heat annealing of the photoelectrode after film deposition can further enhance the performance of the CdSe-sensitized cell. This enhancement was attributed to annealing effect which improves the interfacial connection between TiO_2 and CdSe, as well as the connection among CdSe QDs. An efficiency as high as 2.65% was achieved for the TiO_2/MPTMS/CdSe/ZnS/Heat cell.

Acknowledgments

The support of this research by National Science Council of Taiwan (NSC-98-ET-E006-002-ET and NSC-98-3114-E007-005) and Bureau of Energy, Ministry of Economic Affairs (98-D0204-2) are gratefully acknowledged. Dr. Iván Mora-Seró from Universitat Jaume I, Spain is gratefully acknowledged for his helpful discussion on the EIS spectra.

References

[1] M.K. Nazeeruddin, F. De Angelis, S. Fantacci, A. Selloni, G. Viscardi, P. Liska, S. Ito, B. Takeru, M. Gratzel, J. Am. Chem. Soc. 127 (2005) 16835.
[2] K.G.U. Wijayantha, L.M. Peter, L.C. Otley, Sol. Energy Mater. Sol. Cells 83 (2004) 363.
[3] S.-C. Lin, Y.-L. Lee, C.-H. Chang, Y.-J. Shen, Y.-M. Yang, Appl. Phys. Lett. 90 (2007) 143517.
[4] I. Robel, V. Subramanian, M. Kuno, P.V. Kamat, J. Am. Chem. Soc. 128 (2006) 2385.
[5] R. Plass, S. Pelet, J. Krueger, M. Gratzel, U. Bach, J. Phys. Chem. B 106 (2002) 7578.
[6] P. Hoyer, R. Konenkamp, Appl. Phys. Lett. 66 (1995) 349.
[7] R.D. Schaller, V.I. Klimov, Phys. Rev. Lett. 92 (2004) 186601.
[8] I. Robel, M. Kuno, P.V. Kamat, J. Am. Chem. Soc. 129 (2007) 4136.
[9] Y.-L. Lee, C.-H. Chang, J. Power Sources 185 (2008) 584.
[10] Y.-L. Lee, B.-M. Huang, H.-T. Chien, Chem. Mater. 20 (2008) 6903.
[11] Y.-L. Lee, Y.-S. Lo, Adv. Funct. Mater. 19 (2009) 604.
[12] W.W. Yu, P. Xiaogang, Angew. Chem. Int. Ed. 41 (2002) 2368.
[13] W.W. Yu, L. Qu, W. Guo, X. Peng, Chem. Mater. 15 (2003) 2854.
[14] P. Sudhagar, J.H. Jung, S. Park, R. Sathyamoorthy, H. Ahn, Y.S. Kang, Electrochim. Acta 55 (2009) 113.
[15] I. Mora-Seró, S. Gimeńez, F. Fabregat-Sańtiago, R. Gómez, Q. Shen, T. Toyoda, J. Bisquert, Acc. Chem. Res. 42 (2009) 1848.
[16] S.-M. Yang, C.-H. Huang, J. Zhai, Z.-S. Wang, L. Jiang, J. Mater. Chem. 12 (2002) 1459.
[17] L.J. Diguna, Q. Shen, J. Kobayashi, T. Toyoda, Appl. Phys. Lett. 91 (2007) 023116.